Systematic Study of L-Shell Opacity at Stellar Interior Temperatures

T. Nagayama, J. E. Bailey, G. P. Loisel, G. S. Dunham, G. A. Rochau, C. Blancard, J. Colgan,
Ph. Cossé, G. Faussurier, C. J. Fontes, F. Gilleron, S. B. Hansen, C. A. Iglesias, I. E. Golovkin,
D. P. Kilcrease, J. J. MacFarlane, R. C. Mancini, R. M. More, C. Orban, J.-C. Pain, M. E. Sherrill,
and B. G. Wilson

Systematic study of L-shell opacity at stellar interior temperatures

T. Nagayama[1], J. E. Bailey[1], G. P. Loisel[1], G. S. Dunham[1], G. A. Rochau[1], C. Blancard[2], J. Colgan[3], Ph. Cossé[2], G. Faussurier[2], C. J. Fontes[3], F. Gilleron[2], S. B. Hansen[1], C. A. Iglesias[4], I. E. Golovkin[5], D. P. Kilcrease[3], J. J. MacFarlane[5], R.C. Mancini[6], R. M. More[*,1], C. Orban[7], J.-C. Pain[2], M.E. Sherrill[3], and B.G. Wilson[4]

[1]Sandia National Laboratories, Albuquerque, New Mexico
[2]CEA, DAM, DIF, F-91297 Arpajon, France
[3]Los Alamos National Laboratory, Los Alamos, New Mexico
[4]Lawrence Livermore National Laboratory, Livermore, California
[5]Prism Computational Sciences, Madison, Wisconsin
[6]University of Nevada, Reno, Nevada
[7]Ohio State University, Columbus, Ohio
*Retired from the National Institute for Fusion Science, Toki, Gifu, Japan

The first systematic study of opacity dependence on atomic number at stellar interior temperatures is used to evaluate discrepancies between measured and modeled iron opacity [J. E. Bailey et al, Nature **517**, 56 (2015)]. High-temperature (>180 eV) chromium and nickel opacities are measured with ±6-10% uncertainty, using the same methods employed in the previous iron experiments. The 10-20% experiment reproducibility demonstrates experiment reliability. The overall model-data disagreements are smaller than for iron. However, the systematic study reveals shortcomings in models for density effects, excited states, and open L-shell configurations. The 30-45% underestimate in the modeled short-wavelength quasi-continuum opacity was observed only from iron and only at temperature above 180 eV. Thus, either opacity theories are missing physics that has non-monotonic dependence on the number of bound electrons, or there is an experimental flaw unique to the iron measurement at temperatures above 180 eV.

Opacities quantify photon absorption in matter and are important for high-energy-density (HED) plasma simulations. HED plasma opacity is challenging to calculate and to experimentally validate. Due to lack of benchmark experiments, opacity-calculation accuracy has sometimes been suspected as a source of disagreement between astronomy observations and models. For example, in 1982 Simon requested [1] re-examination of opacity calculations for Cepheid variable stars. In response, new models were developed [2-6] that raised calculated opacities by ~3x for stellar envelopes and resolved the Cepheid variable problem. This precedent, combined with insufficient laboratory experiments to fully test theory, has led to continued speculation that models may underestimate opacity for variable stars [7-9].

Recently, inaccuracy of calculated solar interior opacity was proposed as a potential explanation for disagreement between solar models and helioseismology [10,11]. The opacity at electron temperature $T_e \sim 182$ eV (2.11×10^6 K) and density $n_e \sim 9 \times 10^{22}$ cm^{-3} that exist near the solar convective and radiative zone boundary (CZB) is especially important. To test this hypothesis, frequency-resolved iron opacity was measured at T_e =155-195 eV and $n_e = (7 - 40) \times 10^{21}$ cm^{-3} [12,13] (hereafter BNLR15). The modeled and measured Fe opacities agreed reasonably well at the lowest T_e and n_e, but models under-predict the opacity in several ways as T_e and n_e approach CZB conditions. First, the calculated *quasi-continuum* opacity below 9Å is 30-45% lower than

measured. Second, calculated bound-bound (*BB*) transitions appear stronger and narrower than the measurements. Third, opacity valleys (*windows*) are lower in the calculations. All three discrepancies contribute to lower calculated Rosseland-mean opacity. If the measurements are correct, this explains roughly half the opacity increase needed to resolve the solar problem. However, solving the solar problem ultimately relies on benchmarked opacity *models*. The required opacities for a wide range of elements and conditions cannot be provided by measurements alone. The goal of the work described here is testing hypotheses for the model-data discrepancy.

Hypotheses for the source(s) of the discrepancies fall into two categories: i) there are undetected flaws in the experimental method and/or ii) photon absorption in HED matter is more complex than previously believed. Neither possibility can be ruled out until experiment and theory are reconciled. Experimental [11,14-18] and theoretical investigations [19-24] done up to now have not resolved the discrepancy.

Systematic opacity measurements across atomic number are a powerful way to address this problem. The experiment drives different elements to roughly the same T_e and n_e, but the atom's response to the conditions varies according to the nuclear binding energy. For example, in nickel (Ni:Z=28), electrons are more tightly bound, more difficult to ionize and excite than for iron (Fe:Z=26). Thus, the dominant charge state for Ni is the closed-shell Ne-like configuration [Fig. 1(c)]. In the closed-shell

configurations, angular momentum coupling is appreciably simplified, theory is considered relatively accurate, and opacity is dominated by strong isolated lines. In contrast, as the atomic number is lowered to Fe or to chromium (Cr:Z=24), the dominant charge states shift to open-shell F-like and N-like ions, respectively. These open-shell ions are computationally more challenging and increase opacity complexity. Furthermore, bound-electron wavefunctions of lower-Z elements extend farther from the nucleus and are more easily perturbed by plasma particles. Thus, measuring opacities of Cr, Fe, and Ni not only provides more data to test the experimental platform, but can also help identify possible opacity-model revisions. The value of systematic opacity studies has been recognized for two decades [25,26], but previous experiments were at lower T_e and n_e and did not satisfy benchmark-experiment criteria such as independent plasma diagnostics and reproducibility.

In this letter we describe the first systematic benchmark opacity experiments as a function of atomic number, at stellar interior temperatures. Cr and Ni frequency-resolved opacities were measured. Analysis of co-mixed Mg spectra confirmed that T_e and n_e are nearly the same as those of Fe. Opacities are reproduced within 10-20% from repeated experiments with varied sample thicknesses. Averaging opacity spectra over multiple experiments reduces the uncertainty down to $\pm6\%$ for Cr and $\pm10\%$ for Ni. High reproducibility reflects smallness of experiment-to-experiment errors and demonstrates experiment-method reliability.

Furthermore, the data reveal intriguing atomic-number-dependent disagreements between data and models, which suggest three distinct opacity-model refinements. First, the opacity window disagreement is observed from Cr and Fe, but not from Ni. This suggests a calculational challenge for open L-shell configurations. Second, apparent line-shape disagreements in all three elements suggest insufficient understanding of atomic interaction with plasma environment and/or the treatment of excited states. Third, the modeled quasi-continuum opacity at short wavelength agrees with Cr and Ni measurements, in contrast to the Fe result. The Fe data use the same experimental method and should be as reliable as Cr and Ni. Also, Fe models agreed with lower T_e/n_e measurements. Thus, these Cr, Fe, and Ni quasi-continuum results suggest either models are missing opacity that becomes important at specific conditions that the high T_e/n_e Fe experiments satisfied, or there is an undetected systematic flaw unique to Fe experiments at high T_e/n_e.

Opacity experimental technique has evolved and improved over 30 years [25,27-37]. Typically, frequency-dependent opacity is inferred by measuring transmission through a heated sample. The sample transmission T_ν and opacity κ_ν are related to the source I_0 (backlight) and measured spectra I_ν:

$$T_\nu = I_\nu/I_0 = e^{-\kappa_\nu \rho L}$$

where ρL is the sample areal density.

The measurement requirements are extensive [11,18,32]: (1) The sample is uniformly heated to conditions of interest, achieving local-thermodynamic equilibrium. (2) Spectra (I_0 and I_ν) and sample areal density ρL need to be accurately measured. (3) The instrumental spectral resolving power has to be sufficiently high and accurately measured. (4) Backlight radiation and tamper transmission must be free of short-scale wavelength-dependent structure. (5) Impact of plasma self-emission must be minimized. (6) Tamper-transmission difference [18] must be minimized. (7) Sample temperature, density, and drive radiation must be independently diagnosed. (8) Measurements must be repeated with multiple sample thicknesses to ensure accurate opacity measurements over a wide dynamic range.

The Sandia National Laboratories Z opacity platform (Fig. 1(a)) has been developed over the last decade to meet these criteria [11,12,14,15,38]. The semicircular half-moon sample (i.e., Fe, Cr, or Ni comixed with Mg) is sandwiched between circular low-opacity (CH and/or Be) tamping materials [*tamper,* Fig. 1(b)]. The sample areal density is measured using Rutherford-Backscattering Spectroscopy (RBS) within $\pm4\%$ error. The sample is volumetrically heated by energetic photons from the Z radiation source [34] to achieve uniform, near-equilibrium conditions. At stagnation, the source provides spectrally smooth 350-eV Planckian-like backlight radiation, which overwhelms the 180-eV plasma emission. The sample-attenuated backlight radiation is measured by multiple, slit-imaged, crystal spectrometers fielded along 0° and $\pm9°$ [39] with respect to the sample normal. Each spectrometer records multiple spectrally- and spatially-resolved images with high signal-to-noise ratio (S/N). Thus, each experiment simultaneously records 16 to 36 spectral images that further improves S/N and reduces instrument artifacts. The setup provides sample-attenuated (I_ν at $+9°$) and unattenuated (I_0 at $-9°$) spectra in each experiment.

Continuous investigations since BNLR15 support the experiment reliability. The impact of temporal/spatial gradients, sample/tamper self-emission, and potential difference in tamper transmission at the tamper-only side and opacity-sample-embedded side were numerically investigated and found to be negligible [18]. Uncertainties in the inferred T_e and n_e due to the choice of analysis model have minor impact on the reported model-data disagreements [16]. The validity of the assumed 1-D expansion and the accuracy of RBS areal-density measurements were confirmed by good agreement of the Mg areal density inferred from Mg spectroscopy and that of the RBS measurement.

For further constraints, we performed and repeated six Cr and five Ni opacity experiments with varied sample

thicknesses. The Cr data include four experiments with 3.2×10^{18} and two with 1.8×10^{18} Cr/cm². The Ni data include two experiments with 0.403×10^{18}, and one each with 1.19×10^{18}, 2.30×10^{18}, and 3.74×10^{18} Ni/cm². Plasma conditions inferred from Mg spectroscopy [14] were $T_e = 181 \pm 6 \, (3\%)$ eV and $n_e = (2.9 \pm 0.1) \times 10^{22} \, (3\%)$ cm⁻³ for Cr and $T_e = 187 \pm 6 \, (3\%)$ eV and $n_e = (2.9 \pm 0.3) \times 10^{22} \, (10\%)$ cm⁻³ for Ni.

Checking reproducibility from different sample thicknesses is critical for i) assessing the accuracy of analysis method and ii) confirming reliability of the experimental method. Opacity is most accurately measured when transmission falls in the 0.15-0.85 range [18]. The opacity determination depends on accuracy of transmission determination, background subtraction, and sample areal density in non-linear ways. Fortunately, these uncertainties affect the inferred opacity differently. Their impact depends strongly on the transmission values and thus on the sample thickness. For example, the impact of the background subtraction error (or transmission determination error) on the opacity error depends on the areal density. Thus, any significant systematic errors in those could be identified through thickness-dependence of measured opacity.

Opacity is determined [11,12,13 (supplemental)], including formal propagation of the three uncertainties. Transmission uncertainty is analytically determined from calibration-shot statistics that are collected over a decade. Areal density is known within ±4% based on the RBS measurement and Mg spectroscopy. Line-saturation dependence on backlight brightness suggests a $10\pm3\%$ background exists. The expected opacity values and its uncertainties are determined at every wavelength by propagating these uncertainties using Monte-Carlo methods. Opacities inferred from repeated experiments agree within the inferred uncertainties, supporting the validity of the analysis and uncertainty values.

Furthermore, the small variation in experiment-to-experiment inferred opacity (Fig. 2) reflects the smallness of some systematic errors and all random errors. The excellent reproducibility supports the experiment reliability.

The opacity model OP is widely available and extensively used for solar/stellar models [40]. Comparisons between OP and the opacity measurements (Fig. 3) provide essential clues for model refinements. Over the measured spectral range, opacity is believed to be mostly contributed by bound-bound (BB) transitions ($\kappa_\nu^{BB} \propto \Sigma_l n_l f_{lu} \phi_{lu}(\nu)$) at long wavelengths and bound-free (BF) transitions ($\kappa_\nu^{BF} \propto \Sigma_l n_l \sigma_{lu}(\nu)$) at short wavelengths. n_l is a lower state population; f_{lu} and $\phi_{lu}(\nu)$ are the BB-transition oscillator strength and area-normalized spectral line shape from lower l to upper u states; σ_{lu} is the photoionization cross-section from a state l to an ionized state u. Atomic data calculations affect f_{lu}, σ_{lu}, and BB line locations; population calculations affect

n_l ; density can affect all of these parameters, but especially $\phi_{lu}(\nu)$.

The OP calculation disagrees with measured BB line locations for all three elements, revealing fundamental deficiency in the OP atomic structure. The atomic structure is the basis for accurate calculation of f_{lu}, σ_{lu}, n_l, and $\phi_{lu}(\nu)$, and its deficiency can impact the overall opacity-calculation accuracy.

While OP opacity (Fig. 3) is widely used by astrophysicists due to its accessibility, other opacity models can generate opacities with a more complete set of atomic levels [21,41]. Selected comparisons (Fig. 4) over the BB and window regions with ATOMIC [19], OPAS [42], SCO-RCG [43], SCRAM [44], and TOPAZ [45] show that all these models predict the BB transition energies more accurately than OP. A couple of these models are beginning to be used for detailed solar structure calculations [19,46-51] though their codes are not publicly available. This large collection of models that employ diverse physics approaches can help to identify which physical approximations are most accurate.

The opacity window disagreement trend (Fig. 4, black arrows) suggests that models are challenged by open L-shell configurations, since the disagreement is not observed when ions are predominantly closed shell (i.e., Ni) [see Fig. 1 (c)]. Inaccuracy in wavelengths, strengths, and widths for the multitude of weak BB transitions that arise in open L-shell configurations might lead to windows that are less filled in the model calculations than the data. This hypothesis can be tested by performing Ni experiments at higher temperature, moving the Ni plasma away from the closed-shell electronic configuration.

Calculated line-shape accuracy $\phi_{lu}(\nu)$ is evaluated with the Ne-like Ni 2p-4d line near 9.98Å. This line is used because it is less blended with other lines and has relatively low continuum underneath. The area-normalized line shape for this transition measured in four experiments was reproducible to within 10 % [Fig. 5 (a)]. The two thick-sample measurements were not included in Fig. 5, since the lines are artificially broadened by the combination of the high line-center optical depth, line saturation, and finite instrument resolution. Figure 5(b) shows raw opacity calculations from four opacity models: ATOMIC, OPAS, SCO-RCG, and SCRAM. Some calculations are already after major refinements, motivated by preliminary model-data comparison [58]. The FWHM predictions from these models vary by approximately a factor of 2. These calculated opacities are compared with the measurements by first converting to transmission, convolving with the measured instrumental resolution, and then converting back to opacity. Line shapes $\phi_{lu}(\nu)$ are extracted from the data and calculations by subtracting linear continuum and performing area normalization. While the line widths predicted by most models are significantly underestimated, SCO-RCG predictions agree well with the measured line shape [Fig. 5(c)]. A 60-90%

width increase for the other models is needed to bring them into agreement with the data and with SCO-RCG.

It is reasonable to expect similar width disagreements for other lines since models use the same method for them. Energy is transferred more readily in windows between narrow lines, and therefore narrower lines decrease the calculated mean opacity. In fact, almost all the lines do look broader in the data. However, further scrutiny is necessary to determine accuracy of other line shapes.

The observed line-shape disagreement indicates insufficient understanding of impact collisions by dynamic electrons, the static-ion Stark broadening, and/or satellite lines from excited states. Opacity models commonly compute electron broadening based on the Baranger [52] approximation. The ion Stark effect is neglected or crudely approximated [53], despite a recent publication [24] describing its potential importance. Satellite-line contributions are also computed differently from one model to another. Investigations are underway to identify which aspect of line-broadening theory is responsible for the reported line-shape discrepancies.

The model-data comparison (Fig. 6) over the short-wavelength region shows that the systematically higher quasi-continuum opacity reported by BNLR15 is observed only from Fe. While this proves that the experiments are not always biased to measure higher-than-predicted continuum opacity, the question remains: Why is the predicted iron quasi-continuum lower than the data only for Fe and only at high T_e/n_e [12,13] ?

Currently, there are two hypotheses for this intriguing finding. One is that models miss some important physics that becomes significant at conditions satisfied by the high-T_e/n_e Fe experiments. The BF cross-section has never been experimentally validated for highly ionized ions. Furthermore, the quasi-continuum has significant contribution from billions of weak BB lines from states where multiple bound electrons are in excited orbitals simultaneously [13]. Currently, there is no consensus on how many multi-excited states opacity models should include. The disagreement could also come from some neglected processes. For example, preliminary calculations of two-photon absorption [22] suggest that this neglected process would substantially increase the absorption. Another idea for missing physics was also recently published [54]. Refined calculations need to evaluate whether these suggested contributions are consistent with the entire Cr, Fe, and Ni data set.

The other hypothesis is that there is an undetected error in the high-T_e/n_e Fe-opacity result. According to this hypothesis, the problem must not exist in the Cr, Ni, or lower temperature Fe experiments since the modeled and measured quasi-continuum opacity agreed. This contradicts the assertion that the same methods were used for all the experiments. Nevertheless, it would be valuable to recheck the accuracy of BNLR15 by performing additional high T_e/n_e Fe experiments, as well as revisiting the data analysis.

Ultimately, these complex results demonstrate the power of the systematic opacity study described here. Insisting that models and data should agree over a range of atomic numbers, temperatures, and densities is a powerful test for both opacity theory and experiment. This approach guides more accurate stellar interiors modeling and improved understanding of the internal structure of the Sun.

The implication of our measurements is significant for the sun and many stars. Therefore, the measurements should be confirmed by independent experiments. However, this requires large HED facilities [55-57]. In addition, facility time and resources devoted must be sufficient to satisfy the key criteria reported here, such as high reproducibility and independent plasma diagnostics.

[1]   N. R. Simon, Astrophys. J. **260**, L87 (1982).

[2]   C. A. Iglesias, F. J. Rogers, and B. G. Wilson, Astrophys. J. **322**, L45 (1987).

[3]   C. A. Iglesias, F. J. Rogers, and B. G. Wilson, Astrophys. J. **360**, 221 (1990).

[4]   M. J. Seaton, Y. Yan, D. Mihalas, and A. K. Pradhan, Monthly Notices of the Royal Astronomical Society **266**, 805 (1994).

[5]   F. J. Rogers and C. A. Iglesias, Science **263**, 50 (1994).

[6]   F. J. Rogers and C. A. Iglesias, Space Science Reviews **85**, 61 (1998).

[7]   S. Salmon, J. Montalbán, T. Morel, A. Miglio, M.-A. Dupret, and A. Noels, Monthly Notices of the Royal Astronomical Society **422**, 3460 (2012).

[8]   E. Moravveji, Monthly Notices RAS Letters **455**, L67 (2016).

[9]   A. Hui-Bon-Hoa and S. Vauclair, Astronomy and Astrophysics **610**, L15 (2018).

[10]   S. Basu and H. M. Antia, Physics Reports **457**, 217 (2008).

[11]   J. E. Bailey, G. A. Rochau, R. C. Mancini, C. A. Iglesias, J. J. MacFarlane, I. E. Golovkin, C. Blancard, P. Cosse, and G. Faussurier, Phys. Plasmas **16**, 058101 (2009).

[12]   J. E. Bailey, G. A. Rochau, C. A. Iglesias, J. J. Abdallah, J. J. MacFarlane, I. Golovkin, P. Wang, R. C. Mancini, P. W. Lake, T. C. Moore, M. Bump, O. Garcia, and S. Mazevet, Phys. Rev. Lett. **99**, 265002 (2007).

[13]   J. E. Bailey, T. Nagayama, G. P. Loisel, G. A. Rochau, C. Blancard, J. Colgan, P. Cosse, G. Faussurier, C. J. Fontes, F. Gilleron, I. Golovkin, S. B. Hansen, C. A. Iglesias, D. P. Kilcrease, J. J. MacFarlane, R. C. Mancini, S. N. Nahar, C. Orban, J. C. Pain, A. K. Pradhan, M. Sherrill, and B. G. Wilson, Nature **517**, 56 (2015).

[14]   T. Nagayama, J. E. Bailey, G. Loisel, S. B. Hansen, G. A. Rochau, R. C. Mancini, J. J. MacFarlane, and I. Golovkin, Phys. Plasmas **21**, 056502 (2014).

[15]   T. Nagayama, J. E. Bailey, G. Loisel, G. A. Rochau, and R. E. Falcon, Rev. Sci. Instrum. **85**, 11D603 (2014).

[16]   T. Nagayama, J. E. Bailey, R. C. Mancini, C. A. Iglesias, S. B. Hansen, C. Blancard, H. K. Chung, J. Colgan, P. Cosse, G. Faussurier, R. Florido, C. J. Fontes, F. Gilleron, I. E. Golovkin, D. P. Kilcrease, G. Loisel, J. J. MacFarlane, J. C. Pain, G. A. Rochau, M. E. Sherrill, and R. W. Lee, High Energ. Dens. Phys. **20**, 17 (2016).

[17]   T. Nagayama, J. E. Bailey, G. Loisel, G. A. Rochau, J. J. MacFarlane, and I. Golovkin, Phys. Rev. E **93**, 023202 (2016).

[18]   T. Nagayama, J. E. Bailey, G. P. Loisel, G. A. Rochau, J. J. MacFarlane, and I. E. Golovkin, Phys. Rev. E **95**, 063206 (2017).

[19]   J. Colgan, D. P. Kilcrease, N. H. Magee, M. E. Sherrill, J. J. Abdallah, P. Hakel, C. J. Fontes, J. A. Guzik, and K. A. Mussack, Astrophys. J. **817**, 116 (2016).

[20]   S. N. Nahar and A. K. Pradhan, Phys. Rev. Lett. **116**, 235003 (2016).

[21]   C. A. Iglesias and S. B. Hansen, **835**, 284 (2017).

[22]   R. M. More, S. B. Hansen, and T. Nagayama, High Energ. Dens. Phys. **24**, 44 (2017).

[23]   D. P. Kilcrease, J. Colgan, P. Hakel, C. J. Fontes, and M. E. Sherrill, High Energ. Dens. Phys. **16**, 36 (2015).

[24]   R. C. Mancini, Journal of Physics Conference Series **717**, 012069 (2016).

[25]   G. Winhart, K. Eidmann, C. Iglesias, and A. Bar-Shalom, Phys. Rev. E **53**, R1332 (1996).

[26]   G. Loisel, P. Arnault, S. Bastiani Ceccotti, T. Blenski, T. Caillaud, J. Fariaut, W. Fölsner, F. Gilleron, J. C. Pain, M. Poirier, C. Reverdin, V. Silvert, F. Thais, S. Turck-Chieze, and B. Villette, **5**, 173 (2009).

[27]   S. J. Davidson, J. M. Foster, C. C. Smith, K. A. Warburton, and S. J. Rose, Appl. Phys. Lett. **52**, 847 (1988).

[28]   T. Perry, S. Davidson, F. Serduke, D. Bach, C. Smith, J. Foster, R. Doyas, R. Ward, C. Iglesias, F. Rogers, J. Abdallah, R. Stewart, J. Kilkenny, and R. Lee, Phys. Rev. Lett. **67**, 3784 (1991).

[29]   J. Foster, D. Hoarty, C. Smith, P. Rosen, S. Davidson, S. Rose, T. Perry, and F. Serduke, Phys. Rev. Lett. **67**, 3255 (1991).

[30]   L. Da Silva, B. MacGowan, D. Kania, B. Hammel, C. Back, E. Hsieh, R. Doyas, C. Iglesias, F. Rogers, and R. Lee, Phys. Rev. Lett. **69**, 438 (1992).

[31]   P. Springer, D. Fields, B. Wilson, J. Nash, W. Goldstein, C. Iglesias, F. Rogers, J. Swenson, M. Chen, A. Bar-Shalom, and R. Stewart, Phys. Rev. Lett. **69**, 3735 (1992).

[32]   T. Perry, P. Springer, D. Fields, D. Bach, F. Serduke, C. Iglesias, F. Rogers, J. Nash, M. Chen, B. Wilson, W. Goldstein, B. Rozsynai, R. Ward, J. Kilkenny, R. Doyas, L. Da Silva, C. Back, R. Cauble, S. Davidson, J. Foster, C. Smith, A. Bar-Shalom, and R. Lee, Phys. Rev. E **54**, 5617 (1996).

[33]   P. T. Springer, K. L. Wong, C. A. Iglesias, J. H. Hammer, J. L. Porter, A. Toor, W. H. Goldstein, B. G. Wilson, F. J. Rogers, C. Deeney, D. S. Dearborn, C. Bruns, J. Emig, and R. E. Stewart, J. Quant. Spectrosc. Radiat. Transfer **58**, 927 (1997).

[34]   C. Chenais Popovics, H. Merdji, T. Missalla, F. Gilleron, J. C. Gauthier, T. Blenski, F. Perrot, M. Klapisch, C. Bauche-Arnoult, J. Bauche, A. Bachelier, and K. Eidmann, Astrophys. J. Suppl. Ser. **127**, 275 (2000).

[35]   C. Chenais-Popovics, M. Fajardo, F. Gilleron, U. Teubner, J. C. Gauthier, C. Bauche-Arnoult, A. Bachelier, J. Bauche, T. Blenski, F. Thais, F. Perrot, A. Benuzzi, S. Turck-Chieze, J. P. Chièze, F. Dorchies, U. Andiel, W. Foelsner, and K. Eidmann, Phys. Rev. E **65**, 016413 (2001).

[36]   J. E. Bailey, P. Arnault, T. Blenski, G. Dejonghe, O. Peyrusse, J. J. MacFarlane, R. C. Mancini, M. E. Cuneo, D. S. Nielsen, and G. A. Rochau, J. Quant. Spectrosc. Radiat. Transfer **81**, 31 (2003).

[37]   P. Renaudin, C. Blancard, J. Bruneau, G. Faussurier, J. E. Fuchs, and S. Gary, J. Quant. Spectrosc. Radiat. Transfer **99**, 511 (2006).

[38] J. E. Bailey, G. A. Rochau, R. C. Mancini, C. A. Iglesias, J. J. MacFarlane, I. E. Golovkin, J. C. Pain, F. Gilleron, C. Blancard, P. Cosse, G. Faussurier, G. A. Chandler, T. J. Nash, D. S. Nielsen, and P. W. Lake, Rev. Sci. Instrum. **79**, 113104 (2008).

[39] G. Loisel, J. E. Bailey, G. A. Rochau, G. S. Dunham, L. B. Nielsen-Weber, and C. R. Ball, Rev. Sci. Instrum. **83**, 10E133 (2012).

[40] A. M. Serenelli, Astrophysics and Space Science **328**, 13 (2009).

[41] C. Blancard, J. Colgan, P. Cosse, G. Faussurier, C. J. Fontes, F. Gilleron, I. Golovkin, S. B. Hansen, C. A. Iglesias, D. P. Kilcrease, J. J. MacFarlane, R. M. More, J. C. Pain, M. Sherrill, and B. G. Wilson, Phys. Rev. Lett. **117**, 249501 (2016).

[42] C. Blancard, P. Cossé, and G. Faussurier, Astrophys. J. **745**, 10 (2012).

[43] J.-C. Pain and F. Gilleron, High Energ. Dens. Phys. **15**, 30 (2015).

[44] S. Hansen, J. Bauche, C. Bauche-Arnoult, and M. F. Gu, High Energ. Dens. Phys. **3**, 109 (2007).

[45] C. A. Iglesias, **15**, 4 (2015).

[46] G. Mondet, C. Blancard, P. Cossé, and G. Faussurier, Astrophys. J. Suppl. Ser. **220**, 2 (2015).

[47] M. Le Pennec, S. Turck-Chieze, S. Salmon, C. Blancard, P. Cossé, G. Faussurier, and G. Mondet, Astrophys. J. **813**, L42 (2015).

[48] P. Walczak, C. J. Fontes, J. Colgan, D. P. Kilcrease, and J. A. Guzik, Astronomy and Astrophysics **580**, L9 (2015).

[49] J. Daszyńska-Daszkiewicz, A. A. Pamyatnykh, P. Walczak, J. Colgan, C. J. Fontes, and D. P. Kilcrease, Monthly Notices of the Royal Astronomical Society **466**, 2284 (2017).

[50] G. Buldgen, S. J. A. J. Salmon, M. Godart, A. Noels, R. Scuflaire, M.-A. Dupret, D. R. Reese, J. Colgan, C. J. Fontes, P. Eggenberger, P. Hakel, D. P. Kilcrease, and O. Richard, Monthly Notices RAS Letters **472**, L70 (2017).

[51] G. Buldgen, S. J. A. J. Salmon, A. Noels, R. Scuflaire, D. R. Reese, M.-A. Dupret, J. Colgan, C. J. Fontes, P. Eggenberger, P. Hakel, D. P. Kilcrease, and S. Turck-Chieze, Astronomy and Astrophysics **607**, A58 (2017).

[52] M. Baranger, Phys. Rev. **112**, 855 (1958).

[53] B. F. Rozsnyai, J. Quant. Spectrosc. Radiat. Transfer **17**, 77 (1977).

[54] P. Liu, C. Gao, Y. Hou, J. Zeng, and J. Yuan, Communications Physics 2018 1:1 **1**, 95 (2018).

[55] E. M. Campbell and W. J. Hogan, Plasma Phys. Control. Fusion **41**, B39 (1999).

[56] J.-L. Miquel, C. Lion, and P. Vivini, Journal of Physics Conference Series **688**, 012067 (2016).

[57] N. W. Hopps, T. H. Bett, N. Cann, C. N. Danson, S. J. Duffield, D. A. Egan, S. P. Elsmere, M. T. Girling, E. J. Harvey, D. I. Hillier, D. J. Hoarty, P. M. R. Jinks, M. J. Norman, S. J. F. Parker, P. A. Treadwell, and D. N. Winter, in *High Power Lasers for Fusion Research*, edited by A. A. S. Awwal, A. M. Dunne, H. Azechi, and B. E. Kruschwitz (International Society for Optics and Photonics, 2011), p. 79160C.

[58] T. Nagayama, J. E. Bailey, C. Blancard, J. Colgan, Ph. Cossé, G. Faussurier, C. J. Fontes, F. Gilleron, S. B. Hansen, C. A. Iglesias, D. P. Kilcrease, J. -C. Pain, M. E. Sherrill, B. G. Wilson (private communication)
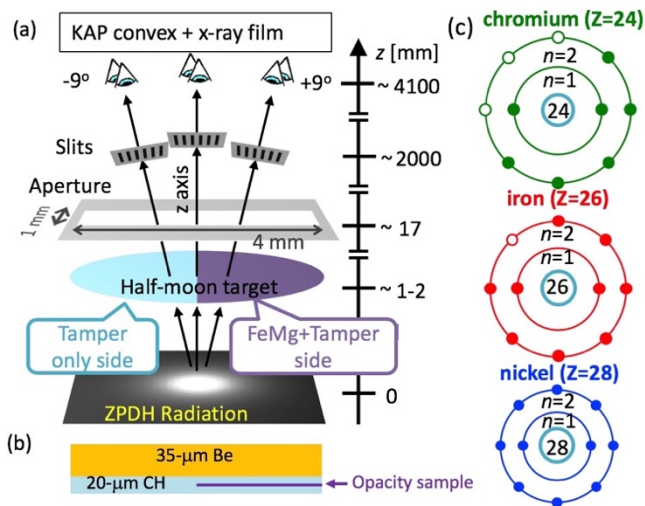
FIG 1. (color) (a) Opacity-experiment setup. (b) Target side view. (c) Dominant electron configurations of Cr, Fe, and Ni at achieved conditions. Vacancies in the shells are indicated by open circles.
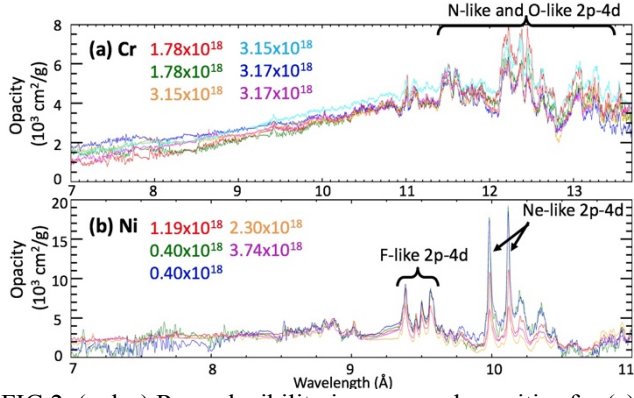
FIG 2. (color) Reproducibility in measured opacities for (a) Cr and (b) Ni. Each color corresponds to independent experiments with their sample areal densities (cm^2/g) embedded in the figure.
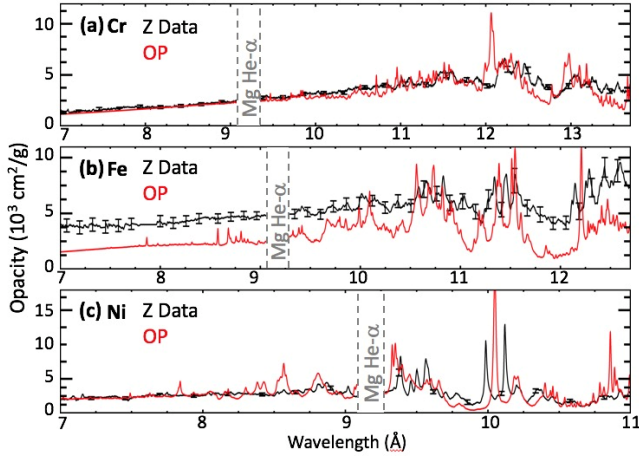
FIG 3. (color) Comparison of OP opacity (red) and measured opacity (black) approximately at 180 eV and 3×10^{22} cm^{-3} for (a) Cr, (b) Fe, and (c) Ni. Fe data and calculation are adopted from Fig. 3 of BNLR15. Opacities over 9.1-9.3 Å depend on the accuracy of Mg He-α removal and are not shown here. Wavelength upper limit is determined by the onset of strong lines from n=2$\rightarrow$3 transitions, which are still under investigation.
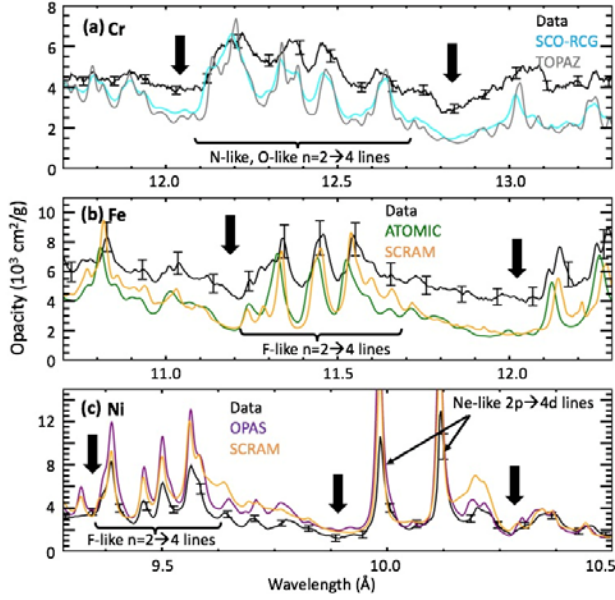
FIG 4. (color) Blow-up comparison of measured (black) and modeled (colored) opacities for (a) Cr, (b) Fe, and (c) Ni over the window and 2p-4d bound-bound lines. While only two models are compared in each plot for clarity, the level of disagreement is similar for all models. The opacity-window (black arrows) disagreement is not observed for Ni, potentially due to closed-L-shell configuration.
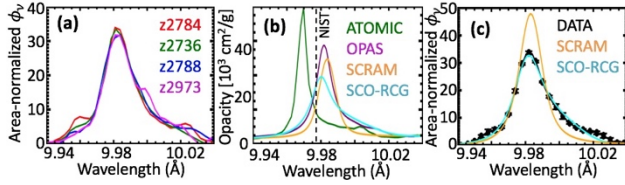

FIG 5. (color) (a) Reproducibility in Ne-like Ni 2p-4d line shapes (b) Model-dependent variation of calculated Ne-like Ni 2p-4d line opacity (without instrument-broadening effects). (c) comparisons of measured (black) and modeled (colored) line shapes (with instrumental transmission resolution; see text). Only the broadest one shows good agreement; other models require 60-90% extra broadening.
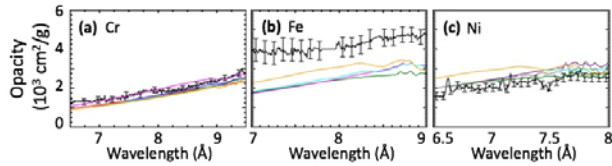

FIG 6. (color) Comparison of measured (black) and modeled (colored) quasi-continuum opacities for (a) Cr, (b) Fe, and (c) Ni, revealing notable discrepancy only from Fe. Models: ATOMIC (green), OPAS (purple), SCO-RCG (cyan), SCRAM (orange), and TOPAZ (gray).